arXiv:1604.04586v1 [cs.SY] 15 Apr 2016

Robust Reduced-Order Model Stabilization for Partial Differential Equations Based on Lyapunov Theory and Extremum Seeking with Application to the 3D Boussinesq Equations

Mouhacine Benosman, Jeff Borggaard, and Boris Kramer

Abstract

We present some results on stabilization for reduced-order models (ROMs) of partial differential equations. The stabilization is achieved using Lyapunov theory to design a new closure model that is robust to parametric uncertainties. The free parameters in the proposed ROM stabilization method are optimized using a model-free multi-parametric extremum seeking (MES) algorithm. The 3D Boussinesq equations provide a challenging numerical test-problem that is used to demonstrate the advantages of the proposed method.

I. Introduction

A well known problem in model reduction for partial differential equations (PDEs) is the so-called *stable model reduction* problem. The goal is to use Galerkin projection onto a suitable set of modes to reduce PDEs to a small system of ordinary differential equations (ODEs), while maintaining the main characteristics of the original model, such as stability and prediction precision.

In this paper, we focus on reduced order models obtained by the method of proper orthogonal decomposition (POD) [1], which has been widely used to obtain surrogate models of tractable size in fluid flow applications. However, it has been observed, e.g., [2]–[6], that POD-ROMs can lose stability. Maintaining stability is crucial for any ROM to be accurate over long time intervals.

We address the stable model reduction problem by using closure models, which are additive, viscosity-like terms introduced in the ROMs to ensure the stability and accuracy of solutions. Through Lyapunov theory, we propose a new closure model that is robust to parametric uncertainties in the model. The obtained closure model has free parameters, which we auto-tune with a model-free MES algorithm to optimally match predictions of the PDE model. The idea of using extremum-seeking to auto-tune closure models has been introduced in [7], however, the difference with this work lies in the new formulation of *robust* closure models. Furthermore, contrary to [7] where the authors considered the simple case of the Burgers' equation, here we study the 3D Boussinesq equations, which is a more challenging test-case and is directly applicable to a number of important control applications [8].

Our work extends existing results in the field. Stable model reduction of Navier-Stokes flow models by adding a nonlinear viscosity term to the reduced-order model is considered in [9]. In [10], [11], incompressible flows are stabilized by an iterative search of the projection modes that satisfy a local Lyapunov stability condition. An optimization-based approach for the POD modes of linear models, which solely focused on matching the outputs of the models is derived in [4], [6]. Kalb and Deane [3] added error correction terms to the reduced-order model for improved accuracy and stabilization. Moreover, the authors in [2] calibrated the POD model by solving a quadratic optimization problem based on three different weighted error norms. Stable model reduction for the Navier-Stokes and Boussinesq equations using turbulence closure models was presented in [12], [13] and [14], respectively. These closure models modify some stability-enhancing coefficients of the reduced-order ODE model using either constant additive terms, such as the constant eddy viscosity model, or time and space varying terms, such as Smagorinsky models. The amplitudes of the additional terms are tuned in such a way to accurately stabilize the reduced-order model.

However, such closure models do not take into account parametric uncertainties in the model, and their tuning is not always straightforward. Our work addresses these issues and proposes a new closure model in Section III that addresses parametric

M. Benosman (m_benosman@ieee.org) is with Mitsubishi Electric Research Laboratories (MERL), Cambridge, MA 02139, USA. Jeff Borggaard is with the the Interdisciplinary Center for Applied Mathematics, Virginia Tech, Blacksburg, VA 24061, USA. B. Kramer is with the Department of Aeronautics and Astronautics, Massachusetts Institute of Technology, Cambridge, MA, 02139, USA.

uncertainties. Furthermore, we achieve optimal auto-tuning of this closure model using a learning-based approach, and is demonstrated using the 3D Boussinesq equations in Section IV. To set the stage, the following section establishes our notation.

II. Basic Notation and Definitions

For a vector $q \in \mathbb{R}^n$, the transpose is denoted by q^*. The Euclidean vector norm for $q \in \mathbb{R}^n$ is denoted by $\|\cdot\|$ so that $\|q\| = \sqrt{q^*q}$. The Frobenius norm of a tensor $A \in \mathbb{R}^{\otimes_i n_i}$, with elements $a_{\mathbf{i}} = a_{i_1 \cdots i_k}$, is defined as $\|A\|_F \triangleq \sqrt{\sum_{\mathbf{i}=\mathbf{1}}^{\mathbf{n}} |a_{\mathbf{i}}|^2}$. The Kronecker delta function is defined as: $\delta_{ij} = 0$, for $i \neq j$ and $\delta_{ii} = 1$. We call a function analytic in a given set, if it admits a convergent Taylor series approximation in some neighborhood of every point of the set. Our PDEs (the Boussinesq equations) are solved on the unit cube $x \in \Omega = (0,1)^3$ and $t \in (0, t_f)$. We shall abbreviate the time derivative by $\dot{f}(t,x) = \frac{\partial}{\partial t} f(t,x)$, and consider the following Hilbert spaces: $\mathcal{H} = L^2(\Omega)$, $\mathcal{V} = H^1_{\text{div}}(\Omega) \subset (\mathcal{H})^3$ for velocity and $\mathcal{T} = H^1(\Omega) \subset \mathcal{H}$ for temperature. Thus, $\mathcal{V}$ is the space of divergence-free vector fields on Ω with components in $H^1(\Omega)$. Dirichlet boundary conditions are also considered in $\mathcal{V}$ and $\mathcal{T}$. We define the inner product $\langle \cdot, \cdot \rangle_{\mathcal{H}}$ and the associated norm $\|\cdot\|_{\mathcal{H}}$ on $\mathcal{H}$ as $\|f\|^2_{\mathcal{H}} = \int_\Omega |f(x)|^2 dx$, and $\langle f, g \rangle_{\mathcal{H}} = \int_\Omega f(x) g(x) dx$, for $f, g \in \mathcal{H}$. A function $T(t,x)$ is in $L^2([0,t_f]; \mathcal{H})$ if for each $0 \leq t \leq t_f$, $T(t,\cdot) \in \mathcal{H}$, and $\int_0^{t_f} \|T(t,\cdot)\|^2_{\mathcal{H}} dt < \infty$ with analogous definitions for the vector valued functions in $(\mathcal{H})^3$. To generalize the discussion below, we consider the abstract Hilbert space $\mathcal{Z}$, and later specialize to $\mathcal{Z} = \mathcal{V} \oplus \mathcal{T}$ when considering the Boussinesq equations. Finally, in the remainder of this paper we consider the stability of dynamical systems in the sense of Lagrange, e.g., [15]: A system $\dot{q} = f(t,q)$ is said to be Lagrange stable if for every initial condition q_0 associated with the time instant t_0, there exists $\epsilon(q_0)$, such that $\|q(t)\| < \epsilon$, $\forall t \geq t_0 \geq 0$.

III. Lyapunov-based robust stable model reduction of PDEs

A. Reduced Order PDE Approximation

We consider a stable dynamical system modeled by a nonlinear partial differential equation of the form

$$\dot{z}(t) = \mathcal{F}(z(t)), \qquad z(0) \in \mathcal{Z}, \tag{1}$$

where $\mathcal{Z}$ is an infinite-dimensional Hilbert space. Solutions to this PDE can be approximated in a finite dimensional subspace $\mathcal{Z}^n \subset \mathcal{Z}$ through expensive numerical discretization, which can be impractical for multi-query settings such as analysis and design, and even more so for real-time applications such as prediction and control. In many systems, including fluid flows, solutions of the PDE may be well-approximated using only a few suitable (optimal) basis functions [1].

This gives rise to reduced-order modeling through Galerkin projection, which can be broken down into three main steps: One first discretizes the PDE using a finite, but large, number of basis functions, such as piecewise quadratic (for finite element methods), higher order polynomials (spectral methods), or splines. In this paper we use the well-established finite element method (FEM), and refer the reader to the large literature, e.g., [16], for details. We denote the approximation of the PDE solution by $z_n(t,\cdot) \in \mathcal{Z}^n$, where $\mathcal{Z}^n$ is an n-dimensional finite element subspace of $\mathcal{Z}$. Secondly, one determines a small set of spatial basis vectors $\phi_i(\cdot) \in \mathcal{Z}^n$, $i = 1, \ldots, r$, $r \ll n$, that well approximates the discretized PDE solution with respect to a pre-specified criterion, i.e.

$$P_n z(t,x) \approx \Phi q(t) = \sum_{i=1}^{r} q_i(t) \phi_i(x). \tag{2}$$

Here, P_n is the projection of $z(t,\cdot)$ onto $\mathcal{Z}^n$, and Φ is a matrix containing the basis vectors $\phi_i(\cdot)$ as column vectors. Note that the dimension n, coming from the high fidelity discretization of the PDE described above, is generally very large, in contrast to the dimension r of the optimal basis set. Thirdly, a Galerkin projection yields a ROM for the coefficient functions $q(\cdot)$ of the form

$$\dot{q}(t) = F(q(t)), \qquad q(0) \in \mathbb{R}^r. \tag{3}$$

The function $F : \mathbb{R}^r \to \mathbb{R}^r$ is obtained using the weak form of the original PDE and Galerkin projection.

The main challenge in this approach lies in the selection of the 'optimal' basis matrix Φ, and the criterion of optimality used. There are many model reduction methods to find those basis functions for nonlinear systems. For example, some of the most used methods are proper orthogonal decomposition (POD) [17], dynamic mode decomposition (DMD) [18], and reduced basis methods (RBM) [19].

Remark 1: We present the idea of closure models in the framework of POD. However, the derivation is not limited to a particular basis. Indeed, these closure models can be applied to ROMs constructed from other basis functions, such as, DMD. The motivation comes from the fact that any low-dimensional basis necessarily removes the ability to represent the smallest

scale structures in the flow and these structures are responsible for energy dissipation. The missing dissipation often must be accounted for with an additional modeling term to ensure accuracy and stability of the ROM.

Remark 2: For our Boussinesq example, we could maintain one set of coefficients for both velocity and temperature [20]. This would be reasonable for the class of free-convection problems considered here. However, to accommodate forced- and mixed-convection problems, we apply the POD procedure below for velocity and temperature data separately. We continue to use the framework in (3) and consider separate basis functions for velocity, $\phi_i = [(\phi_i^{\mathbf{v}})^*; 0^*]^*$ for $i = 1, \ldots, r_{\mathbf{v}}$ and temperature, $\phi_{r_{\mathbf{v}}+i} = [0^*; (\phi_i^T)^*]^*$ for $i = 1, \ldots, r_T$. The different groups of coefficient functions $\{q_i\}_{i=1}^{r_{\mathbf{v}}}$ and $\{q_i\}_{i=r_{\mathbf{v}}+1}^{r_{\mathbf{v}}+r_T}$ (with $r = r_{\mathbf{v}} + r_T$) are associated with the independent variables $\mathbf{v}$ and T, respectively.

B. Proper Orthogonal Decomposition for ROMs

POD-based models are most known for retaining a maximal amount of energy in the reduced model [1], [17]. The POD basis is computed from a collection of s time snapshots

$$\mathcal{S} = \{z_n(t_1, \cdot), ..., z_n(t_s, \cdot)\} \subset \mathcal{Z}^n, \tag{4}$$

of the dynamical system, usually obtained from a discretized approximation of the PDE model in n dimensions. The $\{t_i\}_{i=1}^s$ are time instances at which snapshots are recorded, and do not have to be uniform. The *correlation matrix* K is then defined as

$$K_{ij} = \frac{1}{s}\langle z_n(t_i, \cdot), z_n(t_j, \cdot)\rangle_{\mathcal{H}},\ i, j = 1, ..., s. \tag{5}$$

The normalized eigenvalues and eigenvectors of K are denoted by λ_i and v_i, respectively. Note that the λ_i are also referred to as the *POD eigenvalues*. The ith *POD basis function* is computed as

$$\phi_i(x) = \frac{1}{\sqrt{s}\sqrt{\lambda_i}} \sum_{j=1}^{s} [v_i]_j z_n(t_j, x),\ i = 1, ..., r, \tag{6}$$

where $r \leq \min\{s, n\}$ is the number of retained POD basis functions and depends upon the application. The POD basis functions are orthonormal:

$$\langle \phi_i, \phi_j \rangle_{\mathcal{H}} = \int_\Omega \phi_i(x)^* \phi_j(x) dx = \delta_{ij}, \tag{7}$$

where δ_{ij} denotes the Kronecker delta function.

In this new basis, the solution of the PDE (1) can then be approximated by

$$z_n^{pod}(t, \cdot) = \sum_{i=1}^{r} q_i(t)\phi_i(\cdot)\ \in \mathcal{Z}^n, \tag{8}$$

where $q_i,\ i = 1, ..., r$ are the POD projection coefficients. To find the coefficients $q_i(t)$, the (weak form of the) model (1) is projected onto the rth-order POD subspace $\mathcal{Z}^r \subseteq \mathcal{Z}^n \subset \mathcal{Z}$ using a Galerkin projection in $\mathcal{H}$. In particular, both sides of equation (1) are multiplied by the POD basis functions, where $z(t)$ is replaced by $z_n^{pod}(t) \in \mathcal{Z}^n$, and then both sides are integrated over Ω. Using the orthonormality of the POD basis (7) leads to an ODE of the form (3). A projection of the initial condition for $z(0)$ can be used to determine $q(0)$. The Galerkin projection preserves the structure of the nonlinearities of the original PDE.

C. Closure Models for ROM Stabilization

We continue to present the problem of stable model reduction in its general form, without specifying a particular type of PDE. However, we now assume an affine dependence of the general PDE (1) on a single physical parameter μ,

$$\dot{z}(t) = \mathcal{F}(z(t), \mu), \quad z(0) = z_0 \in \mathcal{Z}, \qquad \mu \in \mathbb{R}, \tag{9}$$

as well as

Assumption 1: The solutions of the original PDE model (9) are assumed to be in $L^2([0, \infty); \mathcal{Z})$, $\forall \mu \in \mathbb{R}$.

We further assume that the parameter μ is critical for the stability and accuracy of the model, i.e., changing the parameter can either make the model unstable, or lead to inaccurate predictions. Since we are interested in fluid dynamics problems, we can consider μ as a viscosity coefficient. The corresponding reduced-order POD model takes the form (3) and (8):

$$\dot{q}(t) = F(q(t), \mu). \tag{10}$$

The issue with this Galerkin POD-ROM (denoted POD-ROM-G) is that the norm of q, and hence z_n^{pod}, might become unbounded at a finite time, even if the solution of (9) is bounded (Lagrange stable).

The main idea behind the closure modeling approach is to replace the viscosity coefficient μ in (10) by a virtual viscosity coefficient μ_{cl}, whose form is chosen to stabilize the solutions of the POD-ROM (10). Furthermore, a penalty term $H(\cdot)$ is added to the original POD-ROM-G, as follows

$$\dot{q}(t) = F(q(t), \mu) + H(q(t)). \tag{11}$$

The term $H(\cdot)$ is chosen depending on the structure of $F(\cdot, \cdot)$ to stabilize the solutions of (11). For instance, one can use the Cazemier penalty model described in [13].

D. Main Result 1: Lyapunov-based Closure Model

Here we introduce the first main result of this paper, namely a Lyapunov-based closure model that is robust to parametric uncertainties. We first rewrite the right-hand side of the ROM model (10) to isolate the linear viscous term as follows,

$$F(q(t), \mu) = \widetilde{F}(q(t)) + \mu\ Dq(t), \tag{12}$$

where $D \in \mathbb{R}^{r \times r}$ represents a constant, negative definite matrix, and the function $\widetilde{F}(\cdot)$ represents the remainder of the ROM model, i.e., the part without damping.

We now consider the case where $\widetilde{F}(\cdot)$ might be unknown, but bounded by a known function. This includes the case of parametric uncertainties in (9) that produce structured uncertainties in (12). To treat this case, we use Lyapunov theory and propose a nonlinear closure model that *robustly* stabilizes the ROM in the sense of Lagrange. Assume that $\widetilde{F}(\cdot)$ satisfies

Assumption 2 (Boundedness of $\widetilde{F}$): The norm of the vector field $\widetilde{F}(\cdot)$ is bounded by a known function of q, i.e., $\|\widetilde{F}(q)\| \leq \widetilde{f}(q)$.

Remark 3: Assumption 2 allows us to consider a general class of PDEs and their associated ROMs. Indeed, all we require is that the right-hand side of (10) can be decomposed as (12), where a linear damping term can be extracted and the remaining nonlinear term $\widetilde{F}$ is bounded. This could allow for more general parametric dependencies and includes many structured uncertainties of the ROM, e.g., a bounded parametric uncertainty can be formulated in this manner.

We now present our first main result.

Theorem 1: Consider the PDE (9) under Assumption 1, together with its stabilized ROM model

$$\dot{q}(t) = \widetilde{F}(q(t)) + \mu_{cl}\ Dq(t) + H(q(t)), \tag{13}$$

where $\widetilde{F}(\cdot)$ satisfies Assumption 2, $D \in \mathbb{R}^{r \times r}$ is negative definite, and μ_{cl} is given by

$$\mu_{cl} = \mu + \mu_e. \tag{14}$$

Here μ is the nominal value of the viscosity coefficient in (9), and μ_e is the additional constant term. Then, the nonlinear closure model

$$H(q) = \mu_{nl} \widetilde{f}(q)\ \mathrm{diag}(d_{11}, ..., d_{rr})\ q, \quad \mu_{nl} > 0 \tag{15}$$

stabilizes the solutions of the ROM to the invariant set

$$\mathcal{S} = \{q \in \mathbb{R}^r\ s.t.\ \mu_{cl} \tfrac{\lambda_{\max}(D)\|q\|}{\widetilde{f}(q)} + \mu_{nl}\|q\| \max\{d_{11}, \ldots, d_{rr}\} + 1 \geq 0\}.$$

Proof 1: First, we prove that the nonlinear closure model (15) stabilizes the ROM (13) to an invariant set. To do so, we use the following energy-like Lyapunov function

$$V(q) = \frac{1}{2} q^* q. \tag{16}$$

We then evaluate the derivative of V along the solutions of (13), and use (15) and Assumption 2 to write

$$\begin{aligned}
\dot{V} &= q^*(\widetilde{F}(q) + \mu_{cl}\ Dq + \mu_{nl}\widetilde{f}(q)\ \mathrm{diag}(d_{11}, ..., d_{rr})\ q) \\
&\leq \|q\|\widetilde{f}(q) + \mu_{cl}\|q\|^2 \lambda_{\max}(D) + \mu_{nl}\widetilde{f}(q)\|q\|^2 \max\{d_{11}, ..., d_{rr}\} \\
&\leq \|q\|\widetilde{f}(q)(1 + \mu_{cl}\frac{\lambda(D)_{\max}\|q\|}{\widetilde{f}(q)} + \mu_{nl} \max\{d_{11}, ..., d_{rr}\}\|q\|).
\end{aligned}$$

This shows convergence to the invariant set $\mathcal{S}$. □

Note that $\lambda_{\max}(D)$ and $\max\{d_{11}, ..., d_{rr}\}$ are negative, thus the sizes of μ_{cl} and μ_{nl} directly influence the size of $\mathcal{S}$. It is also apparent how the use of the term H offers robustness when the uncertainty in $F(\cdot, \cdot)$ is difficult to manage.

E. Main Result 2: MES-based Closure Model Auto-tuning

As discussed in the introduction as well as in [14], tuning the closure model amplitudes is important to achieve an optimal stabilization of the ROM. In this study, we use model-free MES optimization algorithms to tune the coefficients μ_e and μ_{nl} of the closure models presented in Section III-C. An advantage of using MES over other optimization approaches is the auto-tuning capability that such algorithms allow for, as well as their ability to continually tune the closure model, *even during online operation of the system*. Indeed, we first use MES to tune the closure model, but the same algorithm can be coupled to the real system to continually update the closure model coefficients.

Note that MES-based closure model auto-tuning has many advantages. First of all, the closure models can be valid for longer time intervals when compared to standard closure models with constant coefficients that are identified offline over a (fixed) finite time interval. Secondly, the optimality of the closure model ensures that the ROM obtains the most accuracy for a given low-dimensional basis, leading to the smallest possible ROM for a given application.

We begin by defining a suitable learning cost function for the MES algorithm. The goals of the learning (or tuning) are i.) to enforce Lagrange stability of the ROM model (10) and ii.) to ensure that the solutions of the ROM (10) are close to those of the approximation $z_n(t,\cdot)$ to the original PDE (9). The latter learning goal is important for the accuracy of the solution.

We define the learning cost as a positive definite function of the norm of the error between the approximate solutions of (9) and the ROM (11),

$$\begin{aligned} Q(\widehat{\boldsymbol{\mu}}) &= \widetilde{H}(e_z(t,\widehat{\boldsymbol{\mu}})),\\ e_z(t,\widehat{\boldsymbol{\mu}}) &= z_n^{pod}(t,x;\widehat{\boldsymbol{\mu}}) - z_n(t,x;\boldsymbol{\mu}), \end{aligned} \tag{17}$$

where $\widehat{\boldsymbol{\mu}} = [\widehat{\mu}_e, \widehat{\mu}_{nl}]^* \in \mathbb{R}^2$ denotes the learned parameters, and $\widetilde{H}(\cdot)$ is a positive definite function of e_z. Note that the error e_z could be computed offline using solutions of the ROM (11) and approximate solutions of the PDE (9). The error could be also computed online where the $z_n^{pod}(t,x;\widehat{\boldsymbol{\mu}})$ is obtained from solving the model (11) online, but the $z_n(t,x;\boldsymbol{\mu})$ could be replaced by real measurements of the system at selected spatial locations $\{x_i\}$. The latter approach would circumvent the FEM model, and directly operate on the system, making the reduced order model more consistent with respect to the operating plant.

A practical way to implement the MES-based tuning of $\widehat{\boldsymbol{\mu}}$, is to begin with an offline tuning of the closure model. One then uses the obtained ROM (with the optimal values of $\widehat{\boldsymbol{\mu}}$, namely $\boldsymbol{\mu}^{\text{opt}}$) in the online operation of the system, e.g., control and estimation. We can then fine-tune the ROM online by continuously learning the best value of $\widehat{\boldsymbol{\mu}}$ at any given time during the operation of the system.

To derive formal convergence results, we introduce some classical assumptions on the learning cost function.

Assumption 3: The cost function $Q(\cdot)$ in (17) has a local minimum at $\widehat{\boldsymbol{\mu}} = \boldsymbol{\mu}^{\text{opt}}$.

Assumption 4: The cost function $Q(\cdot)$ in (17) is analytic and its variation with respect to $\boldsymbol{\mu}$ is bounded in the neighborhood of $\boldsymbol{\mu}^{\text{opt}}$, i.e., $\|\nabla_{\boldsymbol{\mu}} Q(\widetilde{\boldsymbol{\mu}})\| \leq \xi_2,\ \xi_2 > 0$, for all $\widetilde{\boldsymbol{\mu}} \in \mathcal{N}(\boldsymbol{\mu}^{\text{opt}})$, where $\mathcal{N}(\boldsymbol{\mu}^{\text{opt}})$ denotes a compact neighborhood of $\boldsymbol{\mu}^{\text{opt}}$.

Under these assumptions the following lemma holds.

Lemma 1: Consider the PDE (9) under Assumption 1, together with its ROM model (13), (14), and (15). Furthermore, suppose the closure model amplitudes $\widehat{\boldsymbol{\mu}} = [\mu_e,\ \mu_{nl}]^*$ are tuned using the MES algorithm

$$\begin{aligned} \dot{y}_1(t) &= a_1 \sin\left(\omega_1 t + \frac{\pi}{2}\right) Q(\widehat{\boldsymbol{\mu}}),\\ \widehat{\mu}_e(t) &= y_1 + a_1 \sin\left(\omega_1 t - \frac{\pi}{2}\right),\\ \dot{y}_2(t) &= a_2 \sin\left(\omega_2 t + \frac{\pi}{2}\right) Q(\widehat{\boldsymbol{\mu}}),\\ \widehat{\mu}_{nl}(t) &= y_2 + a_2 \sin\left(\omega_2 t - \frac{\pi}{2}\right), \end{aligned} \tag{18}$$

where $\omega_{\max} = \max(\omega_1, \omega_2) > \omega^{\text{opt}}$, ω^{opt} large enough, and $Q(\cdot)$ is given by (17). Let $e_{\boldsymbol{\mu}}(t) := [{\boldsymbol{\mu}_e}^{\text{opt}} - \widehat{\boldsymbol{\mu}}_e(t), {\boldsymbol{\mu}_{nl}}^{\text{opt}} - \widehat{\boldsymbol{\mu}}_{nl}(t)]^*$ be the error between the current tuned values, and the optimal values $\boldsymbol{\mu}_e^{\text{opt}},\ \boldsymbol{\mu}_{nl}^{\text{opt}}$. Then, under Assumptions 3, and 4, the norm of the distance to the optimal values admits the following bound

$$\|e_{\boldsymbol{\mu}}(t)\| \leq \tfrac{\xi_1}{\omega_{\max}} + \sqrt{a_1^2 + a_2^2},\ t \to \infty, \tag{19}$$

where $a_1,\ a_2 > 0,\ \xi_1 > 0$, and the learning cost function approaches its optimal value within the following upper-bound

$$\|Q(\widehat{\boldsymbol{\mu}}) - Q(\boldsymbol{\mu}^{\text{opt}})\| \leq \xi_2(\tfrac{\xi_1}{\omega} + \sqrt{a_1^2 + a_2^2}), \tag{20}$$

as $t \to \infty$, where $\xi_2 = \max_{\boldsymbol{\mu} \in \mathcal{N}(\boldsymbol{\mu}^{\text{opt}})} \|\nabla_{\boldsymbol{\mu}} Q(\boldsymbol{\mu})\|$.

Proof 2: Based on Assumptions 3, and 4, the extremum seeking nonlinear dynamics (18), can be approximated by a linearly averaged dynamic model (using an averaging approximation over time, [21], p. 435, Definition 1). Furthermore, $\exists\ \xi_1,\ \omega^{\rm opt}$, such that for all $\omega > \omega^{\rm opt}$, the solution of the averaged model $\widehat{\boldsymbol{\mu}}_{\rm aver}(t)$ is locally close to the solution of the original MES dynamics, and satisfies ([21], p. 436)

$$\|\widehat{\boldsymbol{\mu}}(t) - \mathbf{d}(t) - \widehat{\boldsymbol{\mu}}_{\rm aver}(t)\| \leq \tfrac{\xi_1}{\omega},\ \xi_1 > 0,\ \forall t \geq 0,$$

with $\mathbf{d}(t) = [\mathrm{a}_1 \sin(\omega_1 t - \frac{\pi}{2}), \mathrm{a}_2 \sin(\omega_2 t - \frac{\pi}{2})]^*$. Moreover, since $Q(\cdot)$ is analytic it can be approximated locally in $\mathcal{N}(\boldsymbol{\mu}^{\rm opt})$ with a quadratic function, e.g., Taylor series up to second order, which leads to ([21], p. 437)

$$\lim_{t\to\infty} \widehat{\boldsymbol{\mu}}_{\rm aver}(t) = \boldsymbol{\mu}^{\rm opt}.$$

Based on the above, we can write

$$\|\widehat{\boldsymbol{\mu}}(t) - \boldsymbol{\mu}^{\rm opt}\| - \|\mathbf{d}(t)\| \leq \|\widehat{\boldsymbol{\mu}}(t) - \boldsymbol{\mu}^{\rm opt} - \mathbf{d}(t)\| \leq \frac{\xi_1}{\omega},$$

so that

$$\|\widehat{\boldsymbol{\mu}}(t) - \boldsymbol{\mu}^{\rm opt}\| \leq \frac{\xi_1}{\omega} + \|\mathbf{d}(t)\| \quad , t \to \infty,$$

which implies

$$\|\widehat{\boldsymbol{\mu}}(t) - \boldsymbol{\mu}^{\rm opt}\| \leq \frac{\xi_1}{\omega} + \sqrt{a_1^2 + a_2^2},\ \xi_1 > 0,\ t \to \infty.$$

Next, the cost function upper-bound is easily obtained from the previous bound, using the fact that $Q(\cdot)$ is locally Lipschitz, with Lipschitz constant $\xi_2 = \max_{\boldsymbol{\mu}\in\mathcal{N}(\boldsymbol{\mu}^{\rm opt})} \|\nabla_{\boldsymbol{\mu}} Q(\boldsymbol{\mu})\|$. □

IV. The 3D Boussinesq equation

As an example application of our approach, we consider the 3D incompressible Boussinesq equations that describe the evolution of velocity $\mathbf{v}$, pressure p, and temperature T of a fluid. This system serves as a model for the flow of air in a room. The coupled equations reflect the conservation of momentum, mass, and energy, respectively

$$\rho\left(\frac{\partial \mathbf{v}}{\partial t} + \mathbf{v}\cdot\nabla\mathbf{v}\right) = -\nabla p + \nabla\cdot\tau(\mathbf{v}) + \rho\mathbf{g}, \tag{21}$$

$$\nabla\cdot\mathbf{v} = 0, \tag{22}$$

$$\rho c_p\left(\frac{\partial T}{\partial t} + \mathbf{v}\cdot\nabla T\right) = \nabla\left(\kappa\nabla T\right), \tag{23}$$

where the buoyancy force is driven by changes in density $\rho = \rho_0 + \Delta\rho$, and is modeled as perturbations from the nominal temperature T_0 using the perfect gas law $\Delta\rho\mathbf{g} \approx -\rho_0\beta\left(T - T_0\right)\mathbf{g}$, $\beta = 1/T_0$, and the term $\rho_0\mathbf{g}$ is absorbed into the pressure. The viscous stress is $\tau(\mathbf{v}) = \rho\nu\left(\nabla\mathbf{v} + \nabla\mathbf{v}^T\right)$ with kinematic viscosity ν and thermal conductivity κ, and the gravitational acceleration is $\mathbf{g} = -g\widehat{\mathbf{e}}_3$. One typically non-dimensionalizes these equations depending on the application at hand. For this study, we perform non-dimensionalization as follows. By introducing a characteristic length L, characteristic velocity $\mathbf{v}_0$, wall temperature T_w, and defining $\widetilde{x} = \frac{x}{L}$, $\widetilde{t} = \frac{t\mathbf{v}_0}{L}$, $\widetilde{\mathbf{v}} = \frac{\mathbf{v}}{\mathbf{v}_0}$, $\widetilde{p} = \frac{p}{\rho\mathbf{v}_0^2}$, and $\widetilde{T} = \frac{T-T_0}{T_w-T_0}$ we can reduce the number of free parameters to three. These are the Reynolds number $\mathrm{Re} = \frac{\mathbf{v}_0 L}{\nu}$, the Grashof number $\mathrm{Gr} = \frac{g\beta(T_w-T_0)L^3}{\nu^2}$, and the Prandtl number $\mathrm{Pr} = \frac{\nu}{k/\rho c_p}$. Thus,

$$\frac{\partial \mathbf{v}}{\partial t} + \mathbf{v}\cdot\nabla\mathbf{v} = -\nabla p + \nabla\cdot\tau(\mathbf{v}) + \frac{\mathrm{Gr}}{\mathrm{Re}^2} T\,\widehat{\mathbf{e}}_3, \tag{24}$$

$$\nabla\cdot\mathbf{v} = 0, \tag{25}$$

$$\frac{\partial T}{\partial t} + \mathbf{v}\cdot\nabla T = \nabla\cdot\left(\frac{1}{\mathrm{RePr}}\nabla T\right), \tag{26}$$

where $\tau(\mathbf{v}) = \frac{1}{\mathrm{Re}}(\nabla\mathbf{v} + \nabla\mathbf{v}^T)$ and we have dropped the tilde notation.

Following a Galerkin projection onto the subspace spanned by the POD basis functions, the Boussinesq equation is reduced to a POD ROM with the following structure, e.g., [9]

$$\dot{q}(t) = \mu\ D\ q(t) + [Cq(t)]q(t), \tag{27}$$

$$\mathbf{v}(x,t) = \mathbf{v}_0(x) + \sum_{i=1}^{r_{\mathbf{v}}} q_i(t)\phi_i^{\mathbf{v}}(x), \tag{28}$$

$$T(x,t) = T_0(x) + \sum_{i=r_{\mathbf{v}}+1}^{r_T+r_{\mathbf{v}}} q_i(t)\phi_i^{T}(x), \tag{29}$$

where $\mu > 0$ is the viscosity, i.e., the inverse of the Reynolds number, D is a negative definite matrix with diagonal blocks corresponding to the viscous stress and thermal diffusion (scaled by Pr to extract the parameter μ) and C is a three-dimensional tensor corresponding to the convection terms in (24) and (26). Recall the notational setting Remark 2, where we formulated the Boussineq equations in the general framework of (3). We notice that this POD-ROM has mainly a linear term and two quadratic terms, so that it can be written in the form (12), with

$$\widetilde{F}(q) = [Cq]q.$$

If we consider bounded parametric uncertainties for the entries of C, we can write

$$\widetilde{F}(q) = [(C + \Delta C)q]q,$$

where $\|C + \Delta C\|_F \leq c_{\max}$, we have the upper-bound

$$\|\widetilde{F}(q)\| \leq \widetilde{f}(q) \equiv c_{\max}\|q\|^2.$$

In this case the nonlinear closure model (15) is

$$H(q) = \mu_{nl} c_{\max}\|q\|^2 \mathrm{diag}(d_{11}, ..., d_{rr})q, \tag{30}$$

for $\mu_{nl} > 0$ with $d_{ii},\ i = 1, ..., r$ being the diagonal elements of D.

A. Boussinesq equation MES-based POD ROM stabilization

We consider the Rayleigh-Bénard differential-heated cavity problem, modeled with the 3D Boussinesq equations (24)–(26) with the following parameters and boundary conditions. The unit cube was discretized with 495k quadratic tetrahedral elements with 611k nodes leading to 1.83M velocity degrees of freedom and 611k temperature degrees of freedom. Thus, $n \approx 2.4 \times 10^6$. The velocity was taken as zero on the boundary and the temperature was specified at ± 0.5 on the x-faces and taken as homogeneous Neumann on the remaining faces. The non-dimensional parameters were taken as $\mathrm{Re} = 4.964 \times 10^4$, $\mathrm{Pr} = 0.712$, and $\mathrm{Gr} = 7.369 \times 10^7$, reasonable values in a quiet room. The simulation was run from zero velocity and temperature and snapshots were collected to $t_f = 78$ seconds.

We apply the results of Theorem 1 and Lemma 1 to this problem. In this case we use 8 POD basis functions for each variable, for the POD model (POD-ROM-G). The upper bounds on the uncertainties in the matrix and tensor entries are assumed to be $c_{\max} = 10$. The two closure model amplitudes $\widehat{\boldsymbol{\mu}} = [\mu_e, \mu_{nl}]^*$ are tuned using the discrete version of the MES algorithm (18), given by

$$\begin{aligned}
y_1(k+1) &= y_1(k) + a_1\Delta t \sin\left(\omega_1 k\Delta t + \frac{\pi}{2}\right) Q(\widehat{\boldsymbol{\mu}}),\\
\widehat{\mu}_e(k+1) &= y_1(k+1) + a_1\ \sin\left(\omega_1 k\Delta t - \frac{\pi}{2}\right),\\
y_2(k+1) &= y_2(k) + a_2\Delta t \sin\left(\omega_2 k\Delta t + \frac{\pi}{2}\right) Q(\widehat{\boldsymbol{\mu}}),\\
\widehat{\mu}_{nl}(k+1) &= y_2(k+1) + a_2\ \sin\left(\omega_2 k\Delta t - \frac{\pi}{2}\right),
\end{aligned} \tag{31}$$

where $y_1(0) = y_2(0) = 0$, $k = 0, 1, 2, ...$ is the number of learning iterations, and Δt is the time increment. We use MES parameter values: $a_1 = 0.08\ [-]$, $\omega_1 = 10\ [\frac{\mathrm{rad}}{\mathrm{sec}}]$, $a_2 = 10^{-7}\ [-]$, $\omega_2 = 50\ [\frac{\mathrm{rad}}{\mathrm{sec}}]$. The learning cost function is chosen as

$$Q(\boldsymbol{\mu}) = \int_0^{t_f} \langle e_T, e_T\rangle_{\mathcal{H}} dt + \int_0^{t_f} \langle e_{\mathbf{v}}, e_{\mathbf{v}}\rangle_{(\mathcal{H})^3} dt. \tag{32}$$

Moreover, $e_T = P_r T_n - T_n^{pod},\ e_{\mathbf{v}} = P_r \mathbf{v}_n - \mathbf{v}_n^{pod}$ define the errors between the projection of the true model solution onto the POD space $\mathcal{Z}^r$ and the POD-ROM solution for temperature and velocity, respectively.

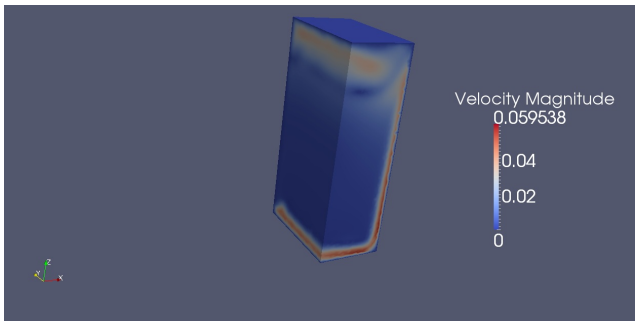

Fig. 1. True velocity profile

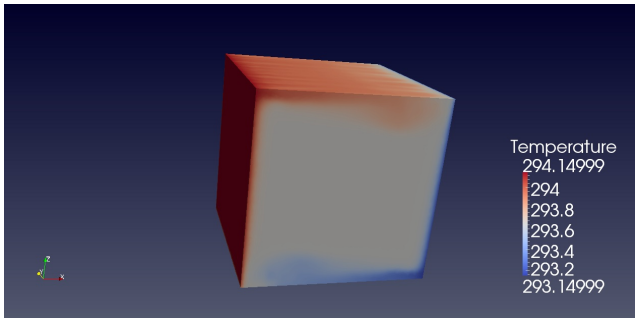

Fig. 2. True temperature profile

We first report in Figures 1, 2 the true velocity and temperature solutions. Figures 3, 4 show the solutions obtained at $t = 50\,\mathrm{sec}$ with the nominal Galerkin ROM, with no closure model. We then report the errors between the true solutions and the POD-ROM-G solutions in Figures 5, and 6.

Next, we show the profile of the learning cost function over the learning iterations in Figure 11. We can see a quick decrease of the cost function within the first 20 iterations. This means that the MES manages to improve the overall solutions of the POD-ROM very quickly. The associated profiles for the two learned closure model amplitudes $\widehat{\mu}_e$ and $\widehat{\mu}_{nl}$ are reported in Figures 12, and 13. We can see that even though the cost function value drops quickly, the MES algorithm continues to fine-tune the values of the parameters $\widehat{\mu}_e$, $\widehat{\mu}_{nl}$ as the simulation proceeds, and eventually reach optimal values of $\widehat{\mu}_e \simeq 0.85$, and $\widehat{\mu}_{nl} \simeq 1.25e-6$ when convergence tolerances are met. We also show the effect of the learning on the POD-ROM solutions by plotting the errors e_T and $e_{\mathbf{v}}$ in Figures 7, 8, 9, 10, which by comparison with Figure 3, 4, 5, 6 show an improvement of the POD-ROM solutions with the MES tuning of the closure models' amplitudes.

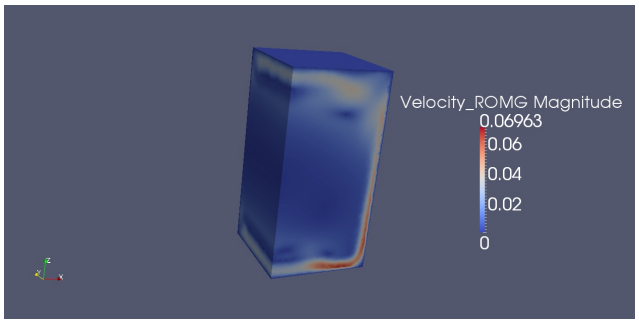

Fig. 3. ROM-G velocity profile

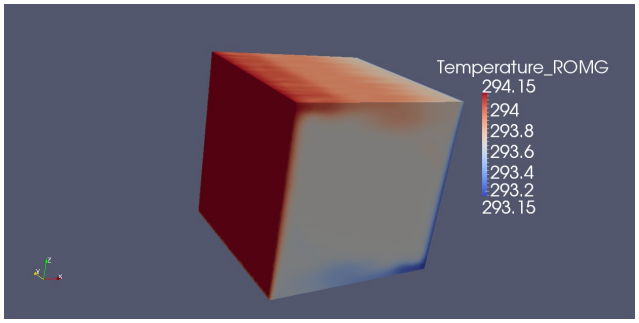

Fig. 4. ROM-G temperature profile

V. Conclusion

In this work we have proposed a new closure model for ROMs that provide robust stabilization when applied to PDEs with parametric uncertainties. We have also proposed the use of a model-free multi-parametric extremum seeking (MES) algorithm to auto-tune the closure model coefficients that optimize the POD-ROM solution predictions. We have validated the proposed method on a challenging 3D Boussinesq test-case by considering a Rayleigh-Bénard differentially-heated cavity problem. The proposed closure model has shown encouraging performance in terms of improving solution precision in the laminar flow cases considered here. Future investigations will be conducted on more challenging flows, e.g., turbulent flows, and online experimental tests using a water-tank test-bed.

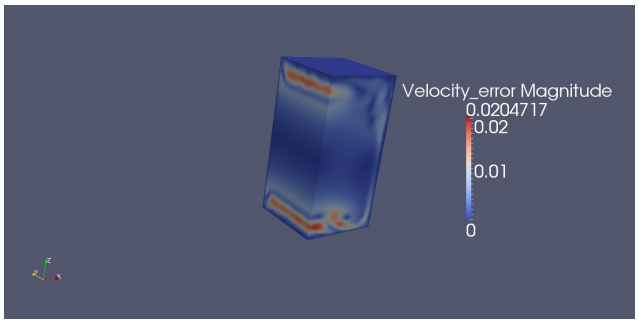

Fig. 5. ROM-G velocity error profile

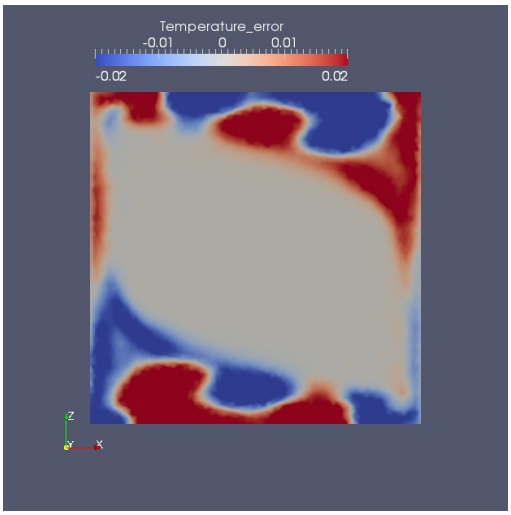

Fig. 6. ROM-G temperature error profile

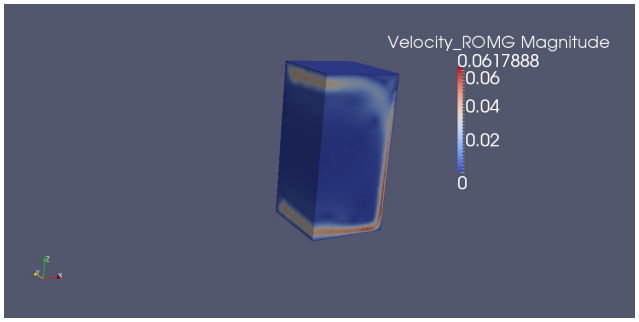

Fig. 7. ROM-G-Learning velocity profile

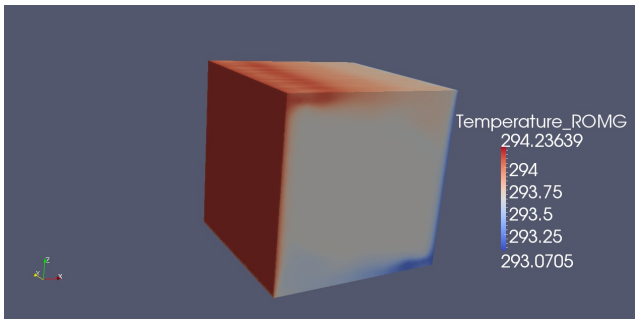

Fig. 8. ROM-G-Learning temperature profile

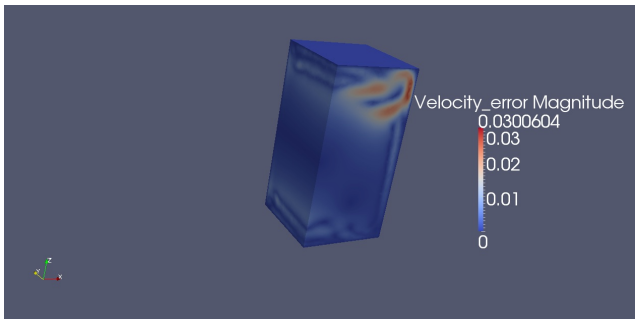

Fig. 9. ROM-G-Learning velocity error profile

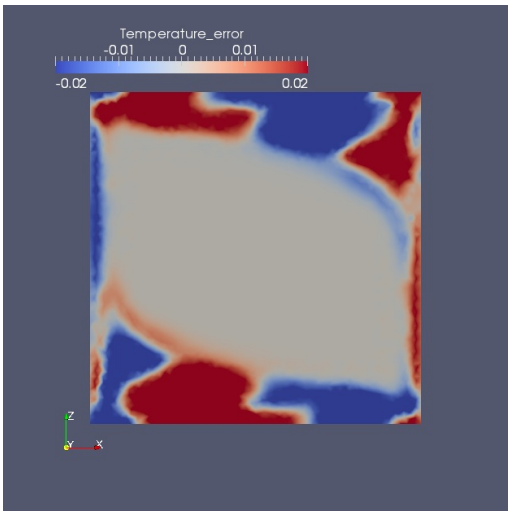

Fig. 10. ROM-G-Learning temperature error profile

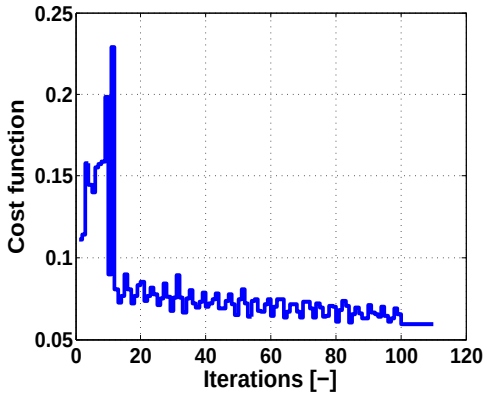

Fig. 11. Learning cost function vs. number of learning iterations

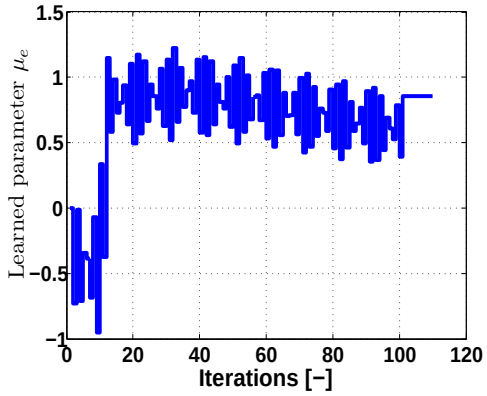

Fig. 12. Coefficient μ_e vs. number of learning iterations

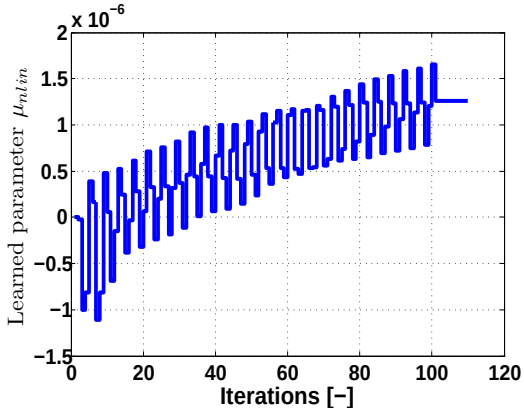

Fig. 13. Coefficient μ_{nl} vs. number of learning iterations

REFERENCES

[1] P. Holmes, J. L. Lumley, and G. Berkooz, *Turbulence, coherent structures, dynamical systems and symmetry*. Cambridge University Press, 1998.

[2] M. Couplet, C. Basdevant, and P. Sagaut, "Calibrated reduced-order POD-Galerkin system for fluid flow modelling," *Journal of Computational Physics*, vol. 207, no. 1, pp. 192–220, 2005.

[3] V. L. Kalb and A. E. Deane, "An intrinsic stabilization scheme for proper orthogonal decomposition based low-dimensional models," *Physics of Fluids*, vol. 19, no. 5, p. 054106, 2007.

[4] T. Bui-Thanh, K. Willcox, O. Ghattas, and B. van Bloemen Waanders, "Goal-oriented, model-constrained optimization for reduction of large-scale systems," *Journal of Computational Physics*, vol. 224, no. 2, pp. 880–896, 2007.

[5] M. Ilak, S. Bagheri, L. Brandt, C. W. Rowley, and D. S. Henningson, "Model reduction of the nonlinear complex Ginzburg-Landau equation," *SIAM Journal on Applied Dynamical Systems*, vol. 9, no. 4, pp. 1284–1302, 2010.

[6] I. Kalashnikova, B. van Bloemen Waanders, S. Arunajatesan, and M. Barone, "Stabilization of projection-based reduced order models for linear time-invariant systems via optimization-based eigenvalue reassignment," *Computer Methods in Applied Mechanics and Engineering*, vol. 272, pp. 251–270, 2014.

[7] M. Benosman, B. Kramer, P. T. Boufounos, and P. Grover, "Learning-based reduced order model stabilization for partial differential equations: Application to the coupled Burgers' equation," in *American Control Conference*, 2016, to appear.

[8] D. Kim, J. Braun, E. M. Cliff and J. Borggaard, "Development, validation and application of a coupled reduced-order CFD model for building control applications," *Building and Environment*, vol. 93, pp. 97–111, 2015.

[9] L. Cordier, B. Noack, G. Tissot, G. Lehnasch, J. Delville, M. Balajewicz, G. Daviller, and R. K. Niven, "Identification strategies for model-based control," *Experiments in Fluids*, vol. 54, no. 1580, pp. 1–21, 2013.

[10] M. Balajewicz, E. Dowell, and B. Noack, "Low-dimensional modelling of high-Reynolds-number shear flows incorporating constraints from the Navier-Stokes equation," *Journal of Fluid Mechanics*, vol. 729, no. 1, pp. 285–308, 2013.

[11] M. Balajewicz, "Lyapunov stable Galerkin models of post-transient incompressible flows," arXiv.org/physics /arXiv:1312.0284, Tech. Rep., December 2013.
[12] Z. Wang, I. Akhtar, J. Borggaard, and T. Iliescu, "Proper orthogonal decomposition closure models for turbulent flows: A numerical comparison," *Computer Methods in Applied Mechanics and Engineering*, vol. 237-240, pp. 10–26, 2012.
[13] O. San and T. Iliescu, "Proper orthogonal decomposition closure models for fluid flows: Burgers equation," *International Journal of Numerical Analyis and Modeling*, vol. 1, no. 1, pp. 1–18, 2013.
[14] O. San and J. Borggaard, "Basis selection and closure for POD models of convection dominated Boussinesq flows," in *21st International Symposium on Mathematical Theory of Networks and Systems*, Groningen, The Netherlands, July 2014, pp. 132–139.
[15] W. Haddad and V. S. Chellaboina, *Nonlinear dynamical systems and control: a Lyapunov-based approach*. Princeton University Press, 2008.
[16] M. Gunzburger, *Finite Element Methods for Viscous Incompressible Flows*. Academic Press, 1989.
[17] K. Kunisch and S. Volkwein, "Galerkin proper orthogonal decomposition methods for a general equation in fluid dynamics," *SIAM Journal on Numerical Analysis*, vol. 40, no. 2, pp. 492–515, 2007.
[18] B. Kramer, P. Grover, P. Boufounos, M. Benosman, and S. Nabi, "Sparse sensing and DMD based identification of flow regimes and bifurcations in complex flows," *arXiv*, 2015.
[19] K. Veroy and A. Patera, "Certified real-time solution of the parametrized steady incompressible Navier-Stokes equations: rigorous reduced-basis a posteriori error bounds," *International Journal for Numerical Methods in Fluids*, vol. 47, no. 8, pp. 773–788, 2005.
[20] B. Podvin and A. Sergent, "Proper orthogonal decomposition investigation of turbulent Rayleigh-Bénard convection in a rectangular cavity," *Physics of Fluids*, vol. 24, no. 105106, 2012.
[21] D. Rempfer, "On low-dimensional Galerkin models for fluid flow," *Theoretical and Computational Fluid Dynamics*, vol. 14, no. 2, pp. 75–88, 2000.